RESEARCH ARTICLE

JBMR®

Single-Cell Transcriptomic Atlas of Parathyroid Adenoma and Parathyroid Carcinoma

Lihui Chen,[1] Ci Shan,[1] Shuqin Xu,[1] Xianzhao Deng,[2] Bomin Guo,[2] Qiong Jiao,[3] Li Zhang,[3] Youben Fan,[2] Hua Yue,[1] and Zhenlin Zhang[1]

[1]Department of Osteoporosis and Bone Disease, Shanghai Clinical Research Center of Bone Disease, Sixth People's Hospital, Shanghai Jiao Tong University School of Medicine, Shanghai, China

[2]Center of Thyroid and Parathyroid, Department of General Surgery, Sixth People's Hospital, Shanghai Jiao Tong University School of Medicine, Shanghai, China

[3]Department of Pathology, Sixth People's Hospital, Shanghai Jiao Tong University School of Medicine, Shanghai, China

ABSTRACT

Primary hyperparathyroidism is typically characterized by monoclonal parathyroid tumors that secrete an excessive amount of parathyroid hormone (PTH). However, the underlying pathogenesis of tumorigenesis remains unclear. We performed single-cell transcriptomic analysis on five parathyroid adenoma (PA) and two parathyroid carcinoma (PC) samples. A total of 63,909 cells were divided into 11 different cell categories; endocrine cells accounted for the largest proportion of cells in both PA and PC, and patients with PC had larger populations of endocrine cells. Our results revealed significant heterogeneity in PA and PC. We identified cell cycle regulators that may play a critical role in the tumorigenesis of PC. Furthermore, we found that the tumor microenvironment in PC was immunosuppressive, and endothelial cells had the highest interactions with other cell types, such as fibroblast-musculature cells and endocrine cells. PC development may be stimulated by fibroblast-endothelial cell interactions. Our study clarifies the transcriptional signatures that underlie parathyroid tumors and offer a potential significant contribution in the study of pathogenesis of PC. © 2023 American Society for Bone and Mineral Research (ASBMR).

KEY WORDS: PARATHYROID ADENOMA; PARATHYROID CARCINOMA; SINGLE-CELL RNA SEQUENCING; PARATHYROID TUMORIGENESIS; TUMOR MICROENVIRONMENT

Introduction

Primary hyperparathyroidism (PHP) is a common endocrine disorder characterized by excessive secretion of parathyroid hormone (PTH) and consequent hypercalcemia, with potential complications in the skeletal, renal, neurocognitive, and cardiovascular systems.[1] Single parathyroid adenomas (PA) account for 80% to 85% of PHP cases, whereas multiglandular parathyroid disease and parathyroid carcinoma (PC) account for 10% to 15% and less than 1% to 5%, respectively.[2,3] Differential diagnosis between adenoma and carcinoma of the parathyroid gland is routinely based on histopathological features, but histopathological differentiation of PC from certain forms of PA is difficult in some cases. In general, these parathyroid tumors are clinically similar, and although our previous study reported that PC patients have higher levels of serum calcium, PTH, and bone turnover markers than PA patients,[4] they cannot be differentiated by preoperative biochemical findings.[5,6] A comprehensive understanding of the genetic, epigenetic, and molecular characteristics of parathyroid tumors is a key step in identifying potential diagnostic biomarkers that can distinguish between different parathyroid tumor types and provide new therapeutic targets and strategies for these rare tumors; however, this remains a challenge in clinical practice.

There are currently no effective tissue markers that can aid in the diagnostic process. Few markers have satisfactory sensitivity and specificity for use in clinical settings. The most commonly used marker in parathyroid tumor diagnostics is the tumor-suppressor protein, parafibromin, encoded by the *CDC73* gene. Loss of parafibromin expression is common in PC but rare in benign tumors.[7] Others such markers are Cyclin D1 and retinoblastoma (Rb). Previous studies have reported that Cyclin D1

(*CCND1*) gene translocation and oncogene action occurred in 8% of adenomas, and its overexpression was observed in 20% to 40% of PA and 90% of malignant PCs.[8] The loss of Rb expression and function is a hallmark of malignancy.[9] The inactivation and allelic deletion of Rb genes have been found to be associated with the development of PC.[10]

Despite extensive research, the underlying developmental origins of PC remain unclear. A Finland-based national retrospective study reported the occurrence of PC in patients with a history of PA between 2000 and 2011,[11] with no evidence of malignant transformation of the original parathyroid adenoma. Another study revealed that the pattern of comparative genomic hybridization (CGH) alterations detected in PC was significantly different from that previously reported in sporadic adenomas, indicating that these two entities may have different pathogeneses.[12] Previous CGH studies of parathyroid tumors showed[13,14] that loss of the 11q13 region was most common in PA, whereas somatic mutations in MEN1 in PC are rare.[15] This implies that PAs developing through the MEN1 pathway do not have a high potential for malignant transformation. However, the genetic basis of sporadic PA, which does not involve the MEN1 locus, remains unknown. Our center[16] performed whole-exome sequencing (WES) on 22 blood-tumor pairs from sporadic PAs and identified the Y54X mutation in the *CDC73* gene, which was previously identified in PCs, and we recently confirmed the presence of somatic mutations in *CDC73* in 6.8% (5/73) of 73 additional sporadic PA samples.[17] This demonstrates that PAs and PCs possess similar molecular signatures. The available results cannot, therefore, be used to establish or exclude a genetic relationship between PA and sporadic PC. As a result, it has not been confirmed whether sporadic PC develops from a benign adenoma or as a separate disease.

The fundamental understanding of the subtle cellular and molecular landscapes in parathyroid tumors remains elusive. Traditional approaches investigate tumors primarily at the bulk-tumor level and have inherent limitations in providing precise information on individual cells residing in a highly admixed tumor microenvironment (TME). Single-cell sequencing technologies have emerged as powerful tools for comprehensively understanding genetic and functional heterogeneity at a single-cell resolution. In this study, we investigated the transcriptomic profiles of 63,909 cells from five parathyroid adenoma and two PC samples. Our study offers a potential significant contribution to the understanding of the pathogenesis of PC at the cellular and molecular levels.

Materials and Methods

Tissue samples

Five parathyroid adenoma and two carcinoma samples were obtained from patients undergoing parathyroidectomy for the management of PHP at the Shanghai Jiao Tong University School of Medicine Affiliated Sixth People's Hospital. Patients with PHP were diagnosed based on persistent hypercalcemia and excess serum PTH.[18] Patients with secondary (eg, vitamin D deficiency, kidney insufficiency, intestinal calcium malabsorption) or tertiary hyperparathyroidism (eg, hyperphosphatemia, renal transplantation) were excluded. All PA patients in this study were newly diagnosed patients. No patient has a PHPT family history. Whole-exome sequencing (WES) of leukocyte DNA was performed and no mutations in common candidate genes of PHPT were detected. None of the patients had an MEN1 mutation or

a history of neck irradiation. All patients met the surgical criteria.[19] After surgical removal, the tumor tissue samples were collected and immediately transferred for tissue preparation. Half of the tissues were subjected to single-cell isolation, while the other half were subjected to immunohistochemistry for the analysis of protein of interest expression. The tumor specimens were diagnosed by professional pathologists according to the 2022 WHO criteria, and the largest single diameter from the pathology report was used as the tumor size.[20] The histological diagnosis of PC is restricted to parathyroid neoplasms that show one of the following[3]: (i) angioinvasion (vascular invasion), (ii) lymphatic invasion, (iii) perineural (or intraneural) invasion, (iv) local malignant invasion into adjacent anatomic structures, or (v) histologically or cytologically documented metastatic disease. This study was approved by the Ethics Committee of Shanghai Jiao Tong University School of Medicine Affiliated Sixth People's Hospital, and informed consent was obtained from all the patients. PA patients have been followed up for a maximum of 2 years and minimum of 1 year so far, and no recurrence of PHP has been detected.

Immunostaining

Tissue specimens were fixed in a 4% neutral formaldehyde solution and then subjected to paraffin embedding, conventional sectioning, and hemotoxylin and eosin (H&E) staining. Light microscopy was performed. Immunohistochemical (IHC) staining was conducted using an automated immunohistochemistry machine (BenchMark@xT; Roche Diagnostics, Mannheim, Germany). The procedure was performed according to the manufacturer's instructions. Primary antibodies against CAM5.2, PTH, CgA, CK19, Ki67, Syn, P53, GATA3, CD34, CD56, and TTF-1 were obtained from Fuzhou Maixin Biotech Co., Ltd. (Fuzhou, China). Anti-HRPT2/parafibromin antibody (catalog #ab223840, RRID: AB_2847816) was diluted at 1:1000. Secondary antibodies were purchased from Roche Diagnostics. IHC staining of Cyclin-D1 (code #IR083), CD45 (catalog #ab40763), CDH1 (catalog #14472 s); c-MYC (catalog #ab32072), TIMP1 (catalog #ab211926) were also performed.

Single-cell RNA statistical analysis

Single-cell RNA sequencing (scRNA-Seq) data analysis was performed by NovelBio Bio-Pharm Technology Co., Ltd. (Shanghai, China) with the NovelBrain Cloud Analysis Platform. To obtain clean data, we used fastp[21] with default parameter filtering of the adaptor sequence and removed low-quality reads to achieve clean data. After that, feature-barcode matrices were obtained by aligning reads to the human genome (GRCh38 Ensemble, version 104) using CellRanger version 6.1.1. We applied the down-sample analysis among samples sequenced according to the mapped barcode reads per cell of each sample and finally achieved the aggregated matrix. Cells containing more than 200 expressed genes and mitochondrial unique molecular identifiers (UMI) rates below 20% passed the cell-quality filtering, and mitochondrial genes were removed from the expression table.

The Seurat package (version 3.1.4, https://satijalab.org/seurat/) was used for cell normalization and regression based on the expression table according to the UMI counts of each sample and percentage of mitochondrial rate to obtain scaled data. The fastMNN function ($k = 10$, $d = 50$, approximate = TRUE) in the R package scran (version 1.12.1) was used to apply the mutual nearest-neighbor method to correct for batch effects among samples.

Utilizing the graph-based cluster method (resolution = 0.8), we acquired the unsupervised cell cluster result based on the principal component analysis's top 10 principal components, and we calculated the marker genes using the FindAllMarkers function with the Wilcoxon rank sum test algorithm under the following criteria: lnFC > 0.25; $p < 0.05$; min.pct > 0.1. To identify the cell types in detail, clusters of the same cell type were selected for cluster analysis, graph-based clustering, and marker analysis.

Single-cell copy-number variation (CNV) evaluation

CNV evaluation of each cell was conducted using the infercnv R package (version 1.4.0; https://github.com/broadinstitute/inferCNV/wiki). The CNVs of all cells were calculated, and the endothelium, fibroblasts, and musculature cells were used as references. The inferCNV analysis was performed with parameters including "denoise," default hidden Markov model (HMM) settings, and a value of 0.1 for cut-off. The default Bayesian latent mixture model with a default threshold value of 0.5 was used to detect the posterior probabilities of CNV alterations in each cell, thereby reducing false-positive CNV calls.

Single-cell regulatory network inference and clustering (SCENIC) analysis

To assess transcription factor (TF) regulation strength, we applied the SCENIC (pySCENIC, v0.9.5)[22] workflow using the 20,000 motif database for RcisTarget and GRNboost. SCENIC consisted of three steps: (i) identification of co-expression modules between TFs and potential target genes; (ii) for each co-expression module, identification of the direct target of the TF by TF-motif enrichment analysis genes, and grouping of each TF and its corresponding direct target gene into a regulon; (iii) scoring each regulon activity for every cell using the AUCell algorithm (AUC).

QuSAGE analysis (gene enrichment analysis)

We used QuSAGE (2.16.1)[23] to characterize the relative activation of a given gene set based on the gene set collected from Kyoto Encyclopedia of Genes and Genomes (KEGG) pathway database, Molecular Signatures Database (http://www.gsea-msigdb.org/gsea/index.jsp), and immune response gene sets from a referenced article.

Gene ontology (GO) functional enrichment

Functional enrichment analysis was performed using GO enrichment analysis (http://www.geneontology.org), and each enriched ontology hierarchy (false discovery rate [FDR] < 0.05) was reported with two terms in the hierarchy: (i) the term with the highest significance value and (ii) the term with the highest specificity.

Pseudo-time analysis

We applied single-cell trajectory analysis utilizing Monocle2 (http://cole-trapnell-lab.github.io/monocle-release) with DDRTree and default parameters. Before Monocle analysis, we selected marker genes from the Seurat clustering results and raw expression counts of the filtered cells. Based on pseudo-time analysis, branch expression analysis modeling was applied for branch fate-determined gene analysis.

Cell communication analysis

To enable systematic analysis of cell–cell communication molecules, we applied cell communication analysis based on CellPhoneDB,[24] a public repository of ligands, receptors, and their interactions. The membrane, secreted, and peripheral proteins of the cluster were annotated at different time points. Based on the interaction and normalized cell matrix achieved by Seurat normalization, a significant mean and cell communication significance ($p < 0.05$) were calculated.

Results

scRNA-seq profiling reveals heterogeneous cell composition in parathyroid tumor tissues

To explore intratumoral heterogeneity in parathyroid tumors, we generated single-cell transcriptome profiles of five parathyroid adenoma samples and two PC samples using the 10x Genomics platform (Fig. 1A). The clinical characteristics and H&E staining results of these patients are presented in Supplemental Table S1 and Supplemental Fig. S1. All samples were evaluated by two pathologists to determine the pathological diagnosis and tumor cellularity (Supplemental Fig. S2 and Supplemental Table S2), and IHC staining of parafibromin was also performed (Supplemental Fig. S3). All samples were mainly composed of chief cells. After initial quality control, single-cell transcriptomes from 63,909 cells were acquired for further analysis (Supplemental Table S3).

By examining variably expressed genes across all cells, we identified 11 major cell types, including endocrine cells (chief cells and oxyphil cells), fibroblasts, and musculature cells, T cells, NK cells, macrophages, dendritic cells (DC), monocytes, mast cells, neutrophils, endothelial cells, and B cells, using uniform manifold approximation and projection (UMAP) analyses (Fig. 1B, C). We then performed differential gene expression analysis to determine the identity of these cell clusters. Each cluster was compared with the other pooled clusters to identify unique gene signatures, and the top 10 significantly differentially expressed (SDE) genes of each cluster are represented in the heat map, as shown in Supplemental Fig. S4. Well-known cell-type markers were used to characterize the cell clusters (Fig. 1D and Supplemental Fig. S5). The epithelial marker EPCAM and parathyroid marker PTH were significantly enriched in the clusters of endocrine cells. Stromal markers, such as DCN, COL6A1, KCNJ8, and ACTA2, were highly expressed in fibroblast and musculature cell clusters. PECAM1 and PLVAP were abundant in endothelial cells. Immune cells were divided into four distinct clusters: T cells, NK cells, B cells, and macrophages. Specific markers were found in each cluster, such as CD3D in T cells and GNLY in NK cells, MS4A1 (also known as CD20), CD79A in B cells, and APOE and C1QA in macrophages. Mast cells were labeled with TPSB2, CPA3, and TPSAB1. Neutrophil cells were labeled with FCGR3B. DCs and monocytes each represented a minor cell population that expressed the CD1C and FCN1 genes, respectively.

We used inferCNV to compare heterogeneity among patients and subtypes based on large-scale somatic CNV events (Fig. 1E). We used endothelium, fibroblasts, and musculature cells as healthy references to estimate the CNVs of PA and PC. Chromosomal amplification (red) and deletion (blue) were mapped to each chromosomal position (column) in all cells (Fig. 1E). These results indicated that the cells obtained large-scale chromosomal CNVs in PC. Endocrine cells in PC exhibited higher CNV levels than in PA (Supplemental Fig. S6).
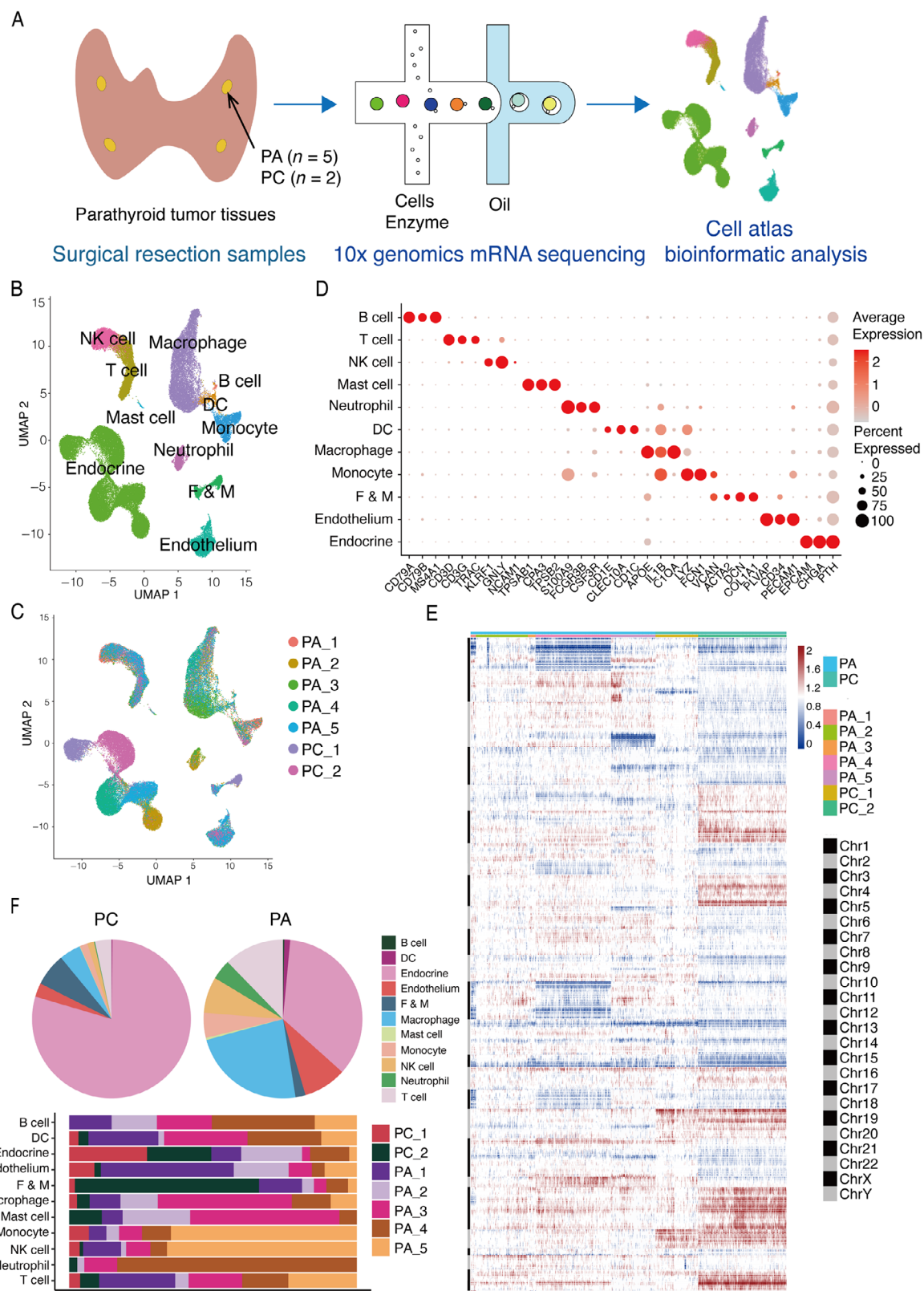
Fig. 1. Overview of the single-cell transcriptomic profile of parathyroid tumor samples. (*A*) Schematic experimental workflow for the study. A total of seven freshly resected parathyroid tumor specimens were collected from seven patients. (*B*) Uniform manifold approximation and projection (UMAP) visualization of 11 major cell types identified and color-coded by their associated clusters. (*C*) UMAP visualization of cells identified and color-coded by each patient. (*D*) Dot plots showing marker genes for 10 distinct cell types. (*E*) The heat map displays large-scale copy number variations (CNVs) of all cells. Red represents gene copy number amplification. (*F*) Bar plots showing the proportion of cell types in each sample. PA = parathyroid adenoma; PC = parathyroid carcinoma.

Each cell cluster contained cells from multiple cases (Fig. 1F). Different parathyroid tumor cases have different proportions of stromal cells. Endocrine cells accounted for the largest proportion of cells in both PAs and PCs. The frequency of cell types varied between PA and PC. For example, compared with PA, patients with PC exhibited an expanded population of endocrine cells, with a frequency of more than 65%. PC tissues were poorly infiltrated by immune cells, and B cells were not observed in the PC tissues. The IHC staining showed that CD45 staining was higher in PA than in PC (Supplemental Fig. S7).

In all cells from our samples, we compared the expression of previously reported PC and PA genes. There were no significant differences in the expression levels of *MYC, KMT2D, EZH2, CDC73, ASXL3, PIK3CA, Rb, CDKN1B, CDKN2B, PRUNE2, mTOR, THRAP3, E2F1,* and *CDKN2A* between PA and PC. Compared with PA, the expression levels of *CCND1, CDKN2C, PTH,* and *CASR* were significantly upregulated in PC ($p < 0.05$), whereas *CDKN1A* expression levels were downregulated ($p < 0.05$).

Distinct molecular features of endocrine cells in parathyroid tumors

To depict their intrinsic portraits, we reclustered all PA and PC endocrine cells and identified 10 main subclusters (endocrine subclusters 0–9) using UMAP analyses (Fig. 2A, B). Endocrine cells from the same case tended to cluster together, indicating a relatively high level of intertumoral heterogeneity. Endocrine cells in subclusters 0 and 5 were mainly derived from PC_2, and endocrine cells in subcluster 3 were mainly derived from PC_1. The unique gene signatures and the top 10 SDE genes of each endocrine subgroup were delineated (Fig. 2C and Supplemental S8). Additionally, gene enrichment analysis (using QuSAGE) was performed to functionally annotate endocrine subgroups (Fig. 2D).

Subcluster 0 showed gene enrichment for the longevity-regulating pathway, neuroactive ligand-receptor interaction, and antigen processing and presentation. *HSPA1A* and *GADD45B* were strongly expressed in cluster 0. TIMP1 was strongly expressed in subclusters 0 and 5. The signature genes of subcluster 3 were enriched with terms related to cell junction, hedgehog signaling pathway, Hippo signaling pathway, and signaling pathways regulating the pluripotency of stem cells. Additionally, hallmark analysis showed that the MYC target pathway was upregulated in subcluster 3 (Fig. 2E and Supplemental Fig. S9). Furthermore, CDH1 and ID2 were strongly expressed in subcluster 3. Overall, subclusters 0, 5, and 3 showed distinct cancer characteristics. Subclusters 1 and 6 are involved in the intestinal immune network for IgA production, indicating that these two groups of cells are active in the immune response. Genes involved in metabolism were elevated in subcluster 2, and subcluster 4 was characterized by extracellular matrix (ECM)-receptor interactions.

We then employed SCENIC to assess the differences in the expression levels of TFs in endocrine cells (Fig. 2F). The TFs BATF, IRF1, and KLF4 were activated in subcluster 0. The analysis of subcluster 1 revealed that STAT3, ETV5, SOX4, and EGR2 had the highest regulatory activity among all regulons, and the TFs ETV5 and SOX4 were also enriched in subcluster 6. Notably, we found that MEIS1, MYC, IRX3, SIX1, ARX, and SIX3 were highly upregulated in subcluster 3.

We assume that PC may have developed from the PA. Pseudotime reconstruction was performed to stratify the tumor cells during cancer development. Endocrine cells from seven cases showed a trajectory that could predict the cancer progression path (Fig. 3A, B). This analysis revealed a branched trajectory with two major branches: cell fate 1 and cell fate 2 (Fig. 3A). Cells from the two patients with PC gathered at different ends; cells from PC_1 and PA_2 constituted most of the cell fate 1 branch. Cells from PC_2 constituted the cell fate 2 branch. Cells from patients with PA accounted for the largest proportion of the pre-branch, which represents the initial state of the tumor cells.

We used IHC staining to examine the expression levels of MYC, CCND1, CDH1, and TIMP1. The four markers' staining was higher in PC than in PA (Fig. 3C).

Role of stromal cells in coordinating the TME in parathyroid tumor

Analysis of stromal cells associated with tumors could provide deeper insights into parathyroid tumor pathophysiology. We examined single-cell transcriptomes of endothelial cells, fibroblast and musculature cells, lymphocytes, and myeloid cells from PA and PC tissues to investigate stromal cell dynamics in the TME.

We detected 4707 ECs and five clusters based on the marker genes (Fig. 4A and Supplemental S10). We then attempted to identify marker genes for each of these clusters and assigned them to known endothelial cell types. These clusters included capillaries, activated capillaries, veins, arteries, and lymphatic endothelial cells. Most endothelial cells belong to PA tissues. Capillary endothelial cells are more common than other cell types in PC tissues. Lymphatic endothelial cells were observed in PC tissues and a few PA tissues. To gain more biological insights into these cells, we used Gene Enrichment Analysis (QuSAGE) to compare the expression profiles of PA and PC endothelial cells (Fig. 4C). The top enriched pathways for PA endothelial cells included ECM-receptor interaction, adherens junction, focal adhesion, the Rap1 signaling pathway, and the PI3K-Akt signaling pathway. Immune-related pathways were enriched for PC endothelial cells. These processes may play a role in the biology of EC. The endothelium represents the primary interface between circulating immune cells and the tumor, which may help explain how ECs contribute to parathyroid tumors.

Fibroblasts are known to be heterogeneous; however, their heterogeneity in parathyroid tumors is unclear.[25] We detected five clusters of fibroblasts, musculature cells, including CD55+ fibroblasts, ACTA2+ fibroblasts, smooth muscle cells and myofibroblasts, inflammatory cancer-associated fibroblasts (iCAFs), and pericytes (Fig. 4B and Supplemental Fig. S10). The iCAFs expressed high levels of CXCL12, DPT, and CXCL14. In our study, iCAFs were mainly observed in PC tissues and a few in the two PA samples, which may indicate that these two PA samples may have some malignant potential. Smooth muscle cells, myofibroblasts (ACTA2, MYH11, and DES), and pericytes (KCNJ8, ABCC9, and CSPG4) were reproducibly detected in PA tissues. CD55+ fibroblasts were observed in one PC and one PA case. QuSAGE analysis comparing fibroblasts from PA and PC tissues showed that cancer-derived fibroblasts were associated with complement and coagulation cascades, the TGF-beta signaling pathway, and the Hippo signaling pathway (Fig. 4D).

Lymphocytes play important roles in inflammation, cancer immune evasion, and responses to immunotherapy treatment.[26] Our data set of 10,413 lymphocytes consisted of 12 clusters, mainly T cells, B cells, and NK cells (Fig. 4E and Supplemental Figs. S10 and S11). We observed that there were few immune cells of all types in PC, and B cells were not detected in PC tissues. T cells are mostly lymphocytes that fall into three T-cell subsets: CD8+ T cells, CD4+ T cells, and CD8−CD4− and gamma delta T
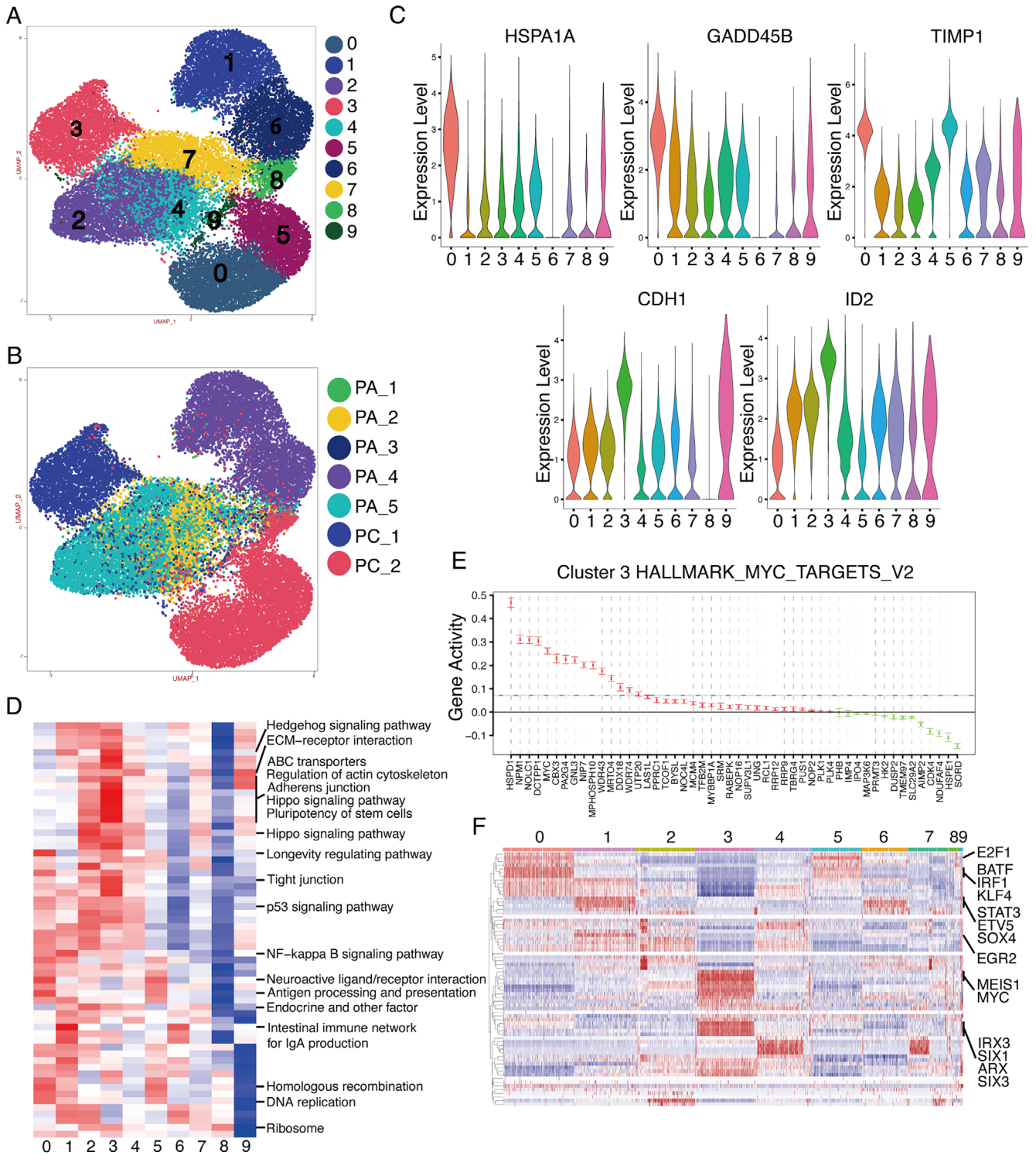
Fig. 2. Characterization of endocrine cells across different patients. (*A*) Uniform manifold approximation and projection (UMAP) visualization of endocrine cell subclustering, color-coded by their associated subclusters. (*B*) UMAP visualization of endocrine cell subclustering by each patient. (*C*) The heat map displays the top 10 SDE genes in each cell subcluster. (*D*) Qusage analysis indicates enriched pathways of each subcluster of endocrine cells. (*E*) Gene activity of genes involved in the MYC-targets pathway in subcluster 3. (*F*) Heat map of gene expression regulation by transcription factors using SCENIC for the endocrine cells. SCENIC = single-cell regulatory network inference and clustering. Source data are provided as a Source Data file.

cells, of which mainly CD8$^+$ T cells were in both PA and PC tissues. The small number of lymphocytes in PC reflects the immunosuppressive state of the TME.

Myeloid cells are essential for the normal functioning of both the innate and adaptive immune systems.[27] We examined the gene signatures of 16 myeloid clusters, including neutrophils,
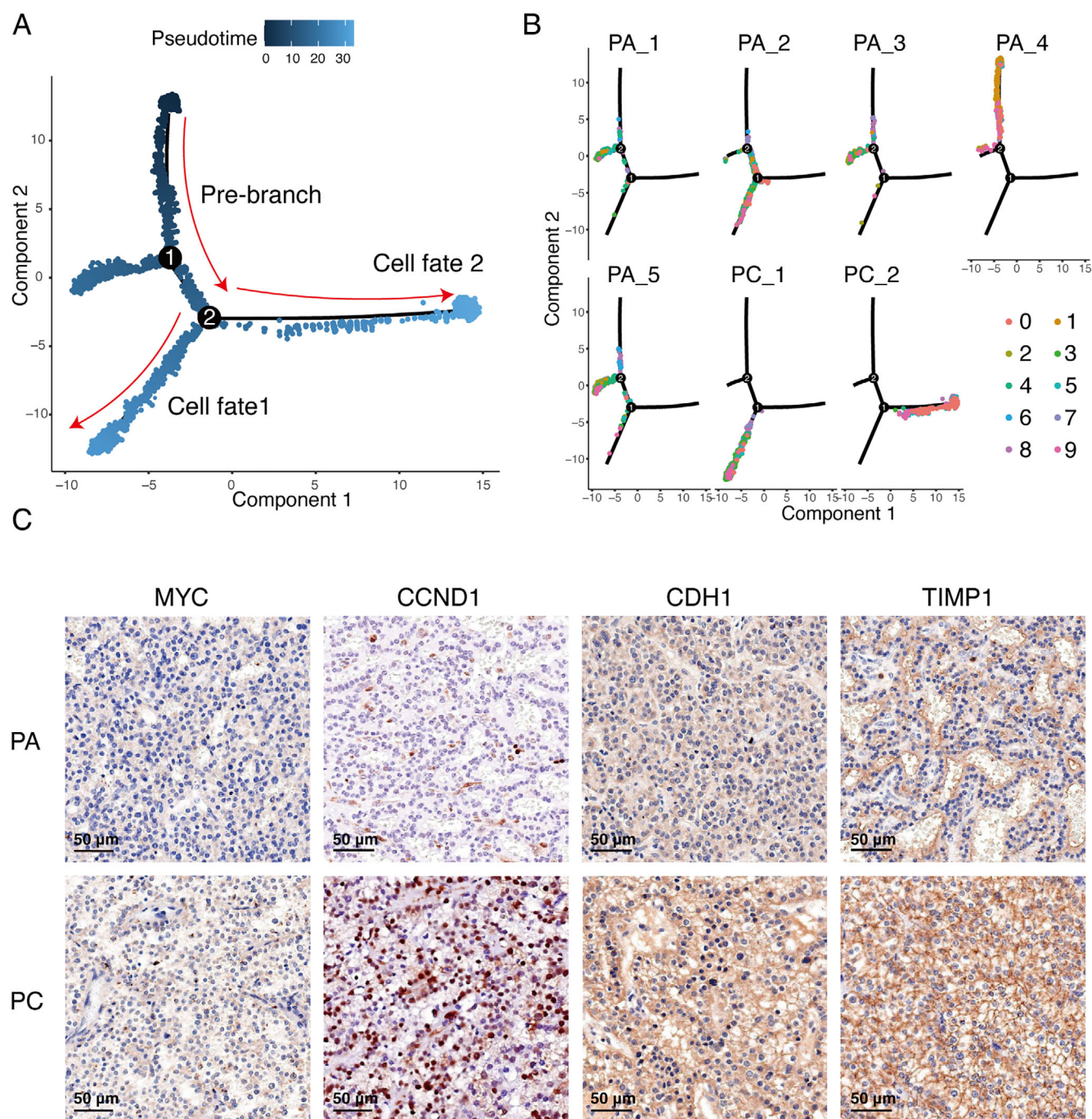
Fig. 3. Gene expression profiles in parathyroid adenoma (PA) and parathyroid carcinoma (PC). (A) The developmental pseudo-time of endocrine cells inferred by analysis with Monocle2. Color key from dark to bright indicates cancer progression from the early to the late stage. (B) Endocrine cells of each patient are shown in the developmental trajectory. (C) Immunohistochemical staining of representative marker genes. Each staining was repeated three times independently on consecutive sections. Scale bars = 50 μm.

monocytes, macrophages, DC, and mast cells (Fig. 4F and Supplemental Figs. S10 and S11). Myeloid cells were mainly observed in PA tissues, and macrophages were mostly myeloid cells belonging to three macrophage subsets: SPP1$^+$ macrophages, NFKB1$^+$ macrophages, and MRC1$^+$ macrophages. SPP1$^+$ macrophages were mainly observed in the PC tissues. We hypothesized that SPP1$^+$ macrophages induce tumor

angiogenesis, promote tumor migration and invasion, and form an immunosuppressive TME in PC.

Cell–cell cross-talk in parathyroid tumors

We used CellPhoneDB to identify the expression of potential cross-talk signaling molecules based on ligand-receptor
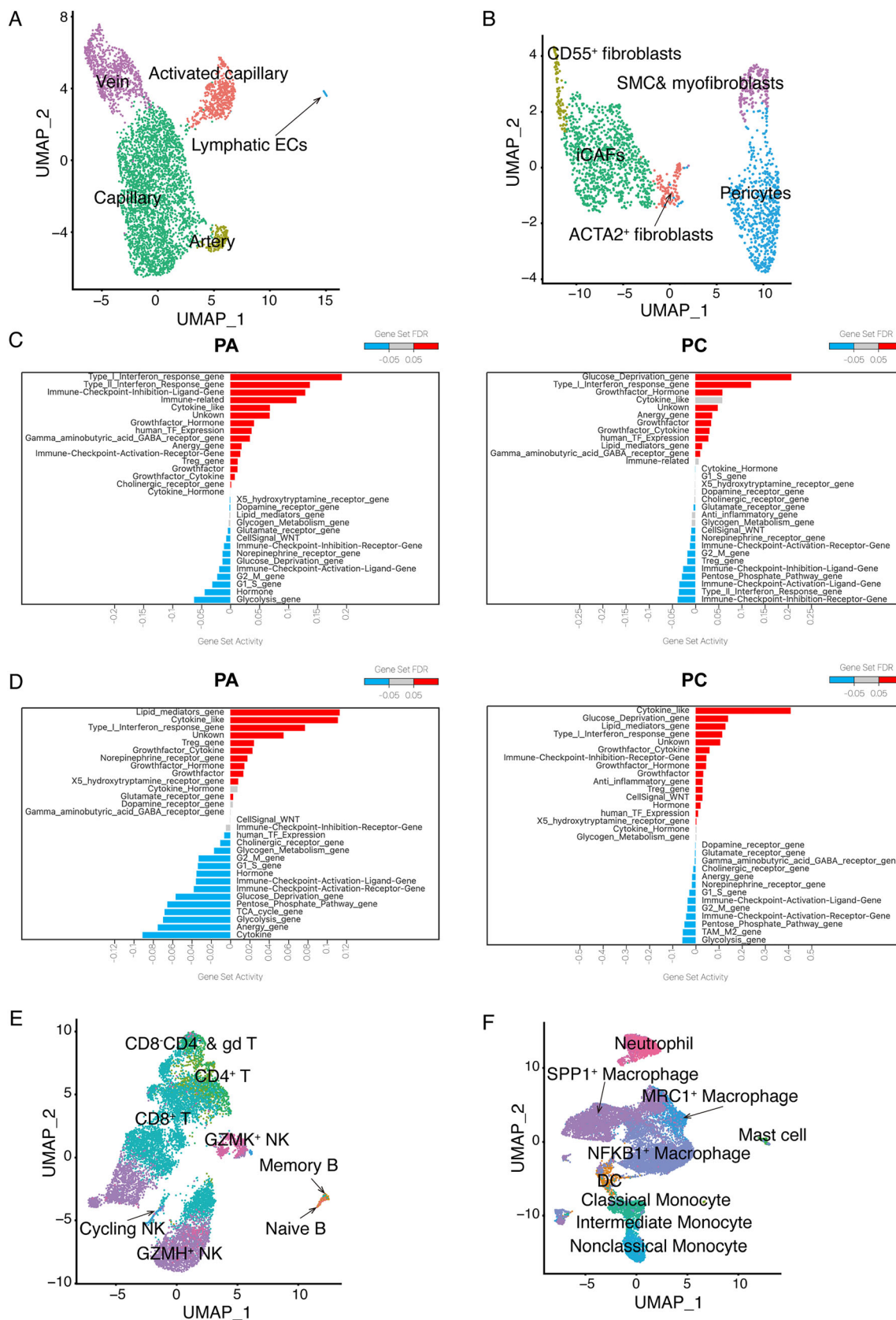
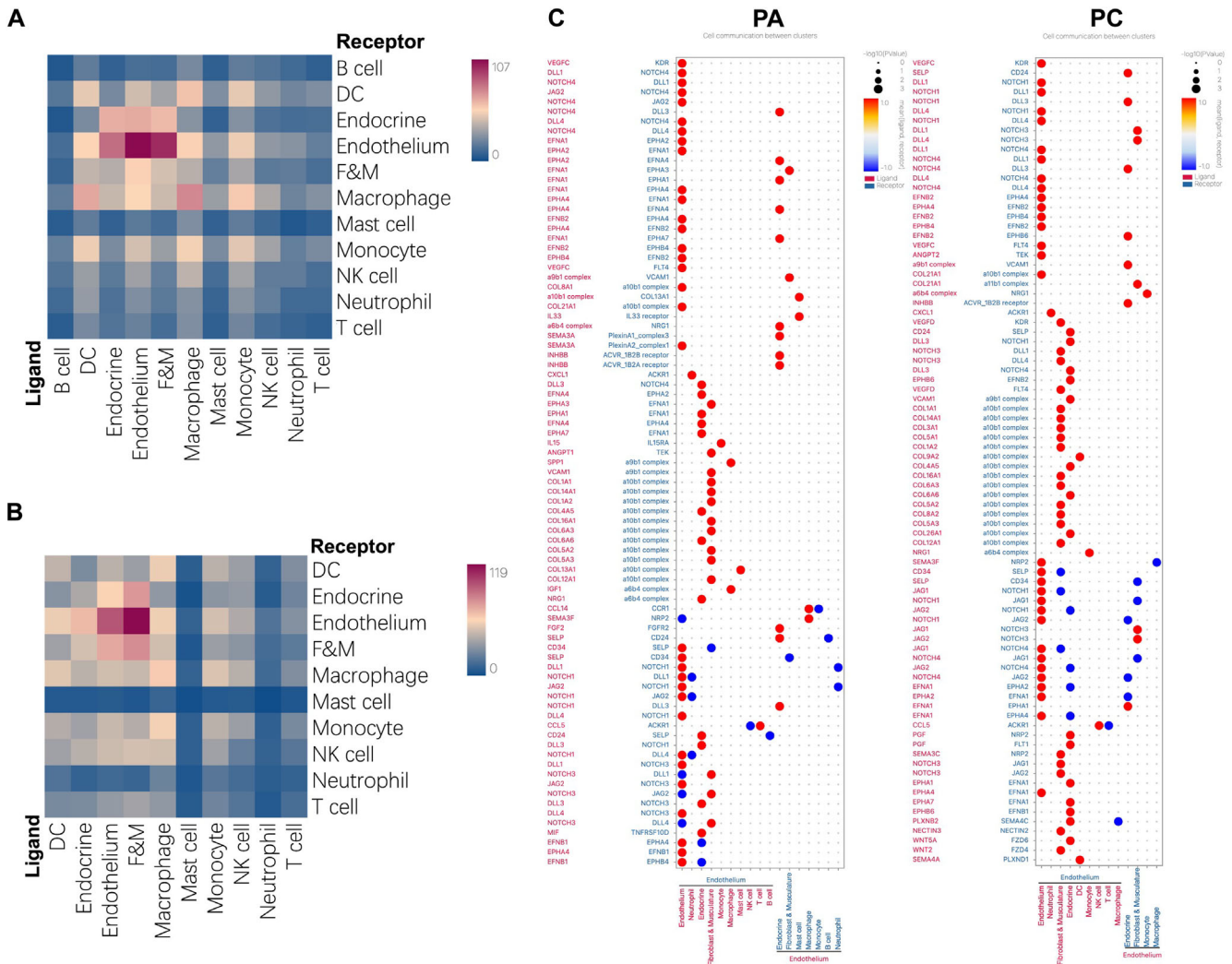*(Figure legend continues on next page.)*

Fig. 5. Cell–cell cross-talk in parathyroid adenoma (PA) and Parathyroid carcinoma (PC). (*A*) Heat map depicting the significant interactions among the 11 major cell types of PA. DC = dendritic cells; F&M = fibroblast and musculature cells. (*B*) Heat map depicting the significant interactions among the 10 major cell types of PC. (*C*) Diagram of the main receptors and ligands expressed on endothelial cells in PA and PC tissues.

interactions. We focused on gene pairs with *p* < 0.001 in strongly interacting cell types. In both PA and PC, endothelial cells showed the most interactions with other cell types, such as fibroblast-musculature cells and endocrine cells (Fig. 5*A, B*). Additionally, we found that the frequency of receptor-ligand interactions between epithelial and fibroblast cells varied markedly when comparing PA with PC samples (Supplemental Fig. S12).

In PC tissues, endothelial cells express high levels of delta-like canonical Notch ligand (DLL) (DLL1 and DLL4) and jagged canonical Notch ligand (JAG)2, which bind to the NOTCH3 receptor expressed by fibroblasts (Fig. 5*C*). Fibroblasts secrete numerous ECM components, including collagens (eg, COL1A1 and COL1A2) and fibronectin (FN1), which bind to integrin receptors (eg, a2b1 complex and a1b1 complex), which are highly

Fig. 4. Profiling stromal and immune cell populations in parathyroid adenoma (PA) and parathyroid carcinoma (PC). (*A*) Uniform manifold approximation and projection (UMAP) visualization of endothelial cell clusters, color-coded by identified cell subtypes; dot plots of selected marker genes in endothelial cell (EC) cluster subtypes. (*B*) UMAP visualization of fibroblast and musculature clusters, color-coded by identified cell subtypes; dot plots of selected marker genes in the fibroblast and musculature cluster subtypes. SMC = smooth muscle cells; SMC & M = smooth muscle cells and myofibroblasts. (*C*) Top enriched pathway of ECs isolated from PA or PC tissues as determined by QuSAGE. (*D*) Top enriched pathway of fibroblast and musculature cells isolated from PA or PC tissues as determined by QuSAGE. (*E*) UMAP visualization of lymphocyte clusters, color-coded by identified cell subtypes; dot plots of selected marker genes in the lymphocyte cluster subtypes. (*F*) UMAP visualization of myeloid cell clusters, color-coded by identified cell subtypes; dot plots of selected marker genes in the myeloid cell cluster subtypes. For UMAP visualization of neutrophil, mast cell, and dendritic cell subclusters, see Supplemental Fig. S10.

Table 1. Comparison of scRNA-seq Analyses Data Between PA and PC Samples

Characteristics	PA	PC
No. of cell type	11	10
Cell type	Endocrine cells, fibroblast & musculature cells, T cells, NK cells, macrophages, DC, monocytes, mast cells, neutrophil, endothelium cells, B cells	Endocrine cells, fibroblast & musculature cells, T cells, NK cells, macrophages, DC, monocytes, mast cells, neutrophil, endothelium cells
Percentage of endocrine cells	32%	77%
Gene expression	—	CCND1↑[a], CDKN2C↑[a], PTH↑[a], CASR↑[a], CDKN1A↓[a]
Level of CNV	Low	High
QuSAGE of endocrine cells	Metabolism and immune-related pathways	Endocrine-related and immune-related pathways
QuSAGE of ECs	ECM-receptor interaction, adherens junction, focal adhesion, Rap1 signaling pathway, and PI3K-Akt signaling pathway	Immune-related pathway
QuSAGE of F&M	Protein digestion and absorption, ECM-receptor interaction, focal adhesion	Complement and coagulation cascades, TGF-beta signaling pathway and Hippo signaling pathway
Immune cells	Many	Few
Cell–cell cross-talk	Fibroblast-endothelial cell interaction	Fibroblast-endothelial cell interaction↑[b]

Abbreviation: CNV = copy number variation; DC = dendritic cells; ECs = endothelial cells; ECM = extracellular matrix; F&M = fibroblast and musculature cells; PA = parathyroid adenoma; PC = parathyroid carcinoma.
[a]Compared with PA.
[b]Higher frequency of receptor-ligand interactions between epithelial and fibroblast cells compared with PA.

expressed by endothelial and endocrine cells (Fig. 5C). Furthermore, the autocrine interaction between the ligands JAG1, JAG2, DLL4, and NOTCH receptors (NOTCH3 and NOTCH4) was highly expressed by endothelial cells in PC (Fig. 5C).

Discussion

There is a scarcity of data on PC because of a lack of sufficient amount and preservation of tissue. We performed high-precision scRNA-seq analyses on PC for the first time and compared them with PA, as there have only been two scRNA-seq studies performed on PA samples thus far[28,29] (Table 1). We identified the 11 major cell types described above in parathyroid tumors and revealed significant heterogeneity between parathyroid adenoma and carcinoma. We suggest that cell cycle regulators may play an important role in parathyroid tumorigenesis. We also identified an immunosuppressive TME in PC.

In the present study, different parathyroid tumor cases had different proportions of stromal cells, and the mutational dynamics were critical for driving PC. Heterogeneity is a typical feature of tumors. Microscopically, parathyroid tumors consist of different proportions of chief, oxyphil, clear, transitional, and cancer cells.[5] Intratumor parathyroid heterogeneity involves tumor cell types as well as tumor cell functions, including PTH synthesis and secretion, and expression patterns of membrane and nuclear receptors.[30] Tumor heterogeneity presents a challenge for understanding the development of parathyroid tumors and cancer treatment.

Endocrine cells account for the largest proportion of parathyroid tumor cells. Patients with PC exhibited an expanded population of endocrine cells compared with those with PA, which is consistent with the clinical phenotype of high PTH levels. In the parathyroid glands, calcium-sensing receptors are present on the surface and regulate serum calcium levels by inhibiting PTH synthesis and secretion. Previous studies have found that CASR expression is decreased in parathyroid tumors,[31,32] which results in insensitivity to the inhibitory feedback of calcium,

altering the calcium-PTH set point and driving parathyroid cell proliferation, suggesting a link to pathogenesis.[31] In contrast to these finding, the CASR gene was found to be more highly expressed in PC than in PA in our study. This is probably because previous studies were performed at the bulk-tumor level, and the cytoplasmic expression of CASR was not precisely assessed. Agarwal and colleagues evaluated 45 parathyroid adenoma and seven carcinoma cases; moderate intensity of cytoplasmic CASR expression was detected in a greater proportion in carcinoma compared with adenoma.[31] The upregulation of the CASR gene in PC may be partly due to its high cytoplasmic expression, which requires further evaluation.

We identified that the regulation of the cell cycle plays an important role in the development of PC. Our study found that TIMP1 and the WNT canonical pathway genes CCND1 and CDH1 were upregulated in PC compared with PA. Previous studies have identified abnormalities in the Wnt/β-catenin signaling pathway in parathyroid tumors.[33] Both parafibromin and CCND1 play important roles in parathyroid tumorigenesis. Parafibromin can downregulate MYC, suggesting its role as a tumor suppressor by inhibiting Wnt signaling.[34] Additionally, parafibromin can suppress CCND1 gene expression,[35] and CCND1 is a target of the Wnt/β-catenin signaling pathway.[36] Overall, these results suggest that the Wnt/β-catenin signaling pathway may play an important role in the development of PC. Another study found the PI3K/AKT/mTOR pathway to be altered in 21% of PC cases.[37] PI3K/Akt/mTOR signaling pathway regulates cell growth and survival during stress.[38] TIMP1 regulates metabolism in metastases by activating the PI3K/Akt pathway.[39] In summary, cell cycle regulators were significantly upregulated in the PC, suggesting that they may play an important role in parathyroid tumorigenesis.

Despite extensive research, the underlying developmental origins of PC remain unclear. We assume that PC may have developed from the PA and our pseudo-time analysis revealed that PC might develop from a benign adenoma. Our previous studies confirmed the presence of somatic mutations in CDC73 in

PA[16,17] and revealed that the novel cancer-related KMT2D genes were the most recurrently altered in a somatic manner.[17] The results of the present scRNA-seq analyses showed no significant difference in the expression levels of CDC73 and KMT2D between PA and PC samples, which proves that PAs and PCs possess similar molecular signatures. But one limitation is that we did not examine normal parathyroid tissue. It is possible that adding normal parathyroid cells might have different results, which needs further study.

The TME is a dynamic and acidified heterocellular location that determines the fate of cancer.[40] In addition to stromal cells, fibroblasts, and endothelial cells, the TME comprises both innate and adaptive immune cells.[41] In our study, fewer endothelial cells were observed in PC tissues, which is consistent with a previous study where PA showed higher microvessel densities compared with normal glands and a low number of vessels in PCs compared with normal glands.[42] Another study also reported that there was no correlation between secretory status and tumor size and angiogenic phenotype, including vascular density and vascular growth factors.[43] This could be due to a partial inhibition of angiogenesis during the transition from benign to neoplastic malignant growth, as well as a high level of vascularization that does not limit activity and growth. There are no data on lymphangiogenesis in PC. A previous study showed that the lymphatic vascular density (LVD) did not differ among normal parathyroid glands, PA, and PHP-related parathyroid hyperplasia.[43] In our study, iCAFs were mainly observed in PC tissues. CXCL12/CXCR4 might play a role in parathyroid tumor angiogenesis and PTH synthesis modulation[25]; therefore, it might be a target for new therapeutic approaches for patients with PHP.

However, data on the immune microenvironment of PC are limited. Consistent with the results of previous studies, our study demonstrated an immunosuppressive TME in PC. Silva and colleagues investigated 17 PCs and 13 atypical parathyroid neoplasms and found that PCs had a lower median CD8+ lymphocyte density than atypical parathyroid neoplasms, which tended to have immune-ignorant and immune-tolerant microenvironments within the neoplasm.[44] Hu and colleagues[45] investigated the relationship between clinical outcomes and tumor-infiltrating immunocytes in samples from 51 Chinese patients with PC by analyzing primary and recurrent/metastatic lesions and found that more tumor-infiltrating immunocytes, more T lymphocytes, and fewer M2 macrophages were correlated with better outcomes and that the immune system is involved in the progression of this endocrine malignancy. Additionally, M2 cells and CAFs act as suppressors of CD8+ lymphocyte infiltration into the core of the tumor[40]; therefore, the small number of lymphocytes and enrichment of SPP1+ macrophages in PC induce tumor angiogenesis, promote tumor migration and invasion, and form an immunosuppressive TME. Considering the limited effect of chemotherapy and radiotherapy on the PC, immunotherapy targeting T cells and tumor-associated macrophages may be promising. Further research on immunotherapies for the treatment of PC is warranted.

Fibroblast-endothelial cell interactions may promote PC development. Activation of the PDGF/PDGFR signaling pathway is associated with cancer proliferation, metastasis, invasion, and angiogenesis by modulating multiple downstream pathways, including the PI3K/AKT and MAPK/ERK pathways.[46] Previous studies have shown that MAPK, Wnt/β-catenin, and PI3K/AKT/mTOR signaling pathways may be associated with parathyroid tumorigenesis and development.[47,48] Collagen overexpression in the TME is linked to enhanced tumor growth and metastasis,

while fibrin contributes to tumorigenesis.[40] Therefore, targeting fibroblast-endothelial cell interactions may be an effective strategy for PC therapy.

Our study has some limitations. First, we did not obtain normal parathyroid tissue and did not compare normal thyroid tissues with PA and PC tissues. Second, as PC is rare, we only collected PC tissue in two cases. To better study the mechanism of parathyroid tumor formation, more cases need to be collected in the future.

In summary, we constructed a single-cell transcriptome atlas for PA and carcinomas. Using this atlas, we characterized the expression patterns of diverse cell types in PA and PC. Notably, our findings suggest that cell cycle regulators may play an important role in the development of PC. In addition, our study showed that there is an immunosuppressive TME in PC. Markers identified in this study are largely unknown and worthwhile for future investigations. In the future, a larger sample size of PCs may help to further clarify and expand on the findings.

Acknowledgments

Author Contributions

Zhenlin Zhang: Designed the study; Writing – review and editing; supervision; methodology. **Lihui Chen:** Conceptualization; data curation; formal analysis; investigation; methodology; validation; visualization; writing – original draft. **Ci Shan:** Methodology; formal analysis; investigation. **Shuqin Xu:** Data curation; validation. **Xianzhao Deng:** Methodology; resources; supervision. **Bomin Guo:** Methodology; resources; supervision. **Qiong Jiao:** Methodology; formal analysis; resources. **Li Zhang:** Methodology; formal analysis; resources. **Youben Fan:** Writing – review and editing; supervision. **Hua Yue:** Writing – review and editing; supervision.

Peer Review

The peer review history for this article is available at https://www.webofscience.com/api/gateway/wos/peer-review/10.1002/jbmr.4824.

Data Availability Statement

The data that support the findings of this study are available from the corresponding author upon reasonable request.

Disclosures

All authors state that they have no conflicts of interest.

References

1. Al Zahrani A, Levine MA. Primary hyperparathyroidism. Lancet. 1997; 349(9060):1233–1238.

2. DeLellis RA. Parathyroid tumors and related disorders. Mod Pathol. 2011;24(Suppl 2):S78–S93.

3. Erickson LA, Mete O, Juhlin CC, Perren A, Gill AJ. Overview of the 2022 WHO classification of parathyroid tumors. Endocr Pathol. 2022;33(1): 64–89.

4. Lin X, Fan Y, Zhang Z, Yue H. Clinical characteristics of primary hyperparathyroidism: 15-year experience of 457 patients in a single center in China. Front Endocrinol (Lausanne). 2021;12:602221.

5. Duan K, Mete O. Parathyroid carcinoma: diagnosis and clinical implications. Turk Patoloji Derg. 2015;31(Suppl 1):80–97.

6. Betea D, Potorac I, Beckers A. Parathyroid carcinoma: challenges in diagnosis and treatment. Ann Endocrinol (Paris). 2015;76(2):169–177.

7. Krebs LJ, Shattuck TM, Arnold A. HRPT2 mutational analysis of typical sporadic parathyroid adenomas. J Clin Endocrinol Metab. 2005;90(9): 5015–5017.

8. Alvelos MI, Mendes M, Soares P. Molecular alterations in sporadic primary hyperparathyroidism. Genet Res Int. 2011;2011:275802.

9. Sellers WR, Kaelin WG Jr. Role of the retinoblastoma protein in the pathogenesis of human cancer. J Clin Oncol. 1997;15(11):3301–3312.

10. Subramaniam P, Wilkinson S, Shepherd JJ. Inactivation of retinoblastoma gene in malignant parathyroid growths: a candidate genetic trigger? Aust N Z J Surg. 1995;65(10):714–716.

11. Ryhanen EM, Leijon H, Metso S, et al. A nationwide study on parathyroid carcinoma. Acta Oncol. 2017;56(7):991–1003.

12. Kytola S, Farnebo F, Obara T, et al. Patterns of chromosomal imbalances in parathyroid carcinomas. Am J Pathol. 2000;157(2):579–586.

13. Palanisamy N, Imanishi Y, Rao PH, Tahara H, Chaganti RS, Arnold A. Novel chromosomal abnormalities identified by comparative genomic hybridization in parathyroid adenomas. J Clin Endocrinol Metab. 1998;83(5):1766–1770.

14. Agarwal SK, Schrock E, Kester MB, et al. Comparative genomic hybridization analysis of human parathyroid tumors. Cancer Genet Cytogenet. 1998;106(1):30–36.

15. Marini F, Giusti F, Iantomasi T, Brandi ML. Parathyroid tumors: molecular signatures. Int J Mol Sci. 2021;22(20):11206.

16. Wei Z, Sun B, Wang ZP, et al. Whole-exome sequencing identifies novel recurrent somatic mutations in sporadic parathyroid adenomas. Endocrinology. 2018;159(8):3061–3068.

17. Tao X, Xu T, Lin X, et al. Genomic profiling reveals the variant landscape of sporadic parathyroid adenomas in Chinese population. J Clin Endocrinol Metab. 2023:dgad002.

18. Walker MD, Silverberg SJ. Primary hyperparathyroidism. Nat Rev Endocrinol. 2018;14(2):115–125.

19. Wilhelm SM, Wang TS, Ruan DT, et al. The American Association of Endocrine Surgeons Guidelines for Definitive Management of Primary Hyperparathyroidism. JAMA Surg. 2016;151(10):959–968.

20. Lampen-Sachar K, Zhao BS, Zheng JT, et al. Correlation between tumor measurement on computed tomography and resected specimen size in lung adenocarcinomas. Lung Cancer. 2012;75(3): 332–335.

21. Chen S, Zhou Y, Chen Y, Gu J. Fastp: an ultra-fast all-in-one FASTQ preprocessor. Bioinformatics. 2018;34(17):i884–i890.

22. Aibar S, Gonzalez-Blas CB, Moerman T, et al. SCENIC: single-cell regulatory network inference and clustering. Nat Methods. 2017;14(11): 1083–1086.

23. Yaari G, Bolen CR, Thakar J, Kleinstein SH. Quantitative set analysis for gene expression: a method to quantify gene set differential expression including gene-gene correlations. Nucleic Acids Res. 2013; 41(18):e170.

24. Vento-Tormo R, Efremova M, Botting RA, et al. Single-cell reconstruction of the early maternal-fetal interface in humans. Nature. 2018; 563(7731):347–353.

25. Verdelli C, Vaira V, Corbetta S. Parathyroid tumor microenvironment. Adv Exp Med Biol. 2020;1226:37–50.

26. Hegmans JPJJ, Aerts JGJV. Immunomodulation in cancer. Curr Opin Pharmacol. 2014;17:17–21.

27. Gabrilovich DI, Ostrand-Rosenberg S, Bronte V. Coordinated regulation of myeloid cells by tumours. Nat Rev Immunol. 2012;12(4): 253–268.

28. Zhang X, Hu Y, Cui M, et al. Cell diversity and immune infiltration in parathyroid tumour microenvironment. Endocr Relat Cancer. 2023; 30(3):e220325.

29. Lu S, Chen X, Gong M, et al. Single-cell RNA sequencing reveals the role of cell heterogeneity in the sex difference in primary hyperparathyroidism. Front Endocrinol (Lausanne). 2023;14:1165890.

30. Verdelli C, Tavanti GS, Corbetta S. Intratumor heterogeneity in human parathyroid tumors. Histol Histopathol. 2020;35(11):1213–1228.

31. Agarwal S, Kardam S, Chatterjee P, et al. CaSR expression in normal parathyroid and PHPT: new insights into pathogenesis from an autopsy-based study. J Endocrinol Invest. 2022;45(2):337–346.

32. Storvall S, Leijon H, Ryhanen EM, et al. Filamin a and parafibromin expression in parathyroid carcinoma. Eur J Endocrinol. 2021;185(6): 803–812.

33. Bjorklund P, Akerstrom G, Westin G. An LRP5 receptor with internal deletion in hyperparathyroid tumors with implications for deregulated WNT/beta-catenin signaling. PLoS Med. 2007;4(11):e328.

34. Mosimann C, Hausmann G, Basler K. Parafibromin/hyrax activates Wnt/Wg target gene transcription by direct association with beta-catenin/armadillo. Cell. 2006;125(2):327–341.

35. Woodard GE, Lin L, Zhang JH, Agarwal SK, Marx SJ, Simonds WF. Parafibromin, product of the hyperparathyroidism-jaw tumor syndrome gene HRPT2, regulates cyclin D1/PRAD1 expression. Oncogene. 2005;24(7):1272–1276.

36. Shtutman M, Zhurinsky J, Simcha I, et al. The cyclin D1 gene is a target of the beta-catenin/LEF-1 pathway. Proc Natl Acad Sci USA. 1999; 96(10):5522–5527.

37. Pandya C, Uzilov AV, Bellizzi J, et al. Genomic profiling reveals mutational landscape in parathyroid carcinomas. JCI Insight. 2017;2(6): e92061.

38. Porta C, Paglino C, Mosca A. Targeting PI3K/Akt/mTOR signaling in cancer. Front Oncol. 2014;4:64.

39. Song GH, Xu SF, Zhang H, et al. TIMP1 is a prognostic marker for the progression and metastasis of colon cancer through FAK-PI3K/AKT and MAPK pathway. J Exp Clin Canc Res. 2016;35(1):148.

40. Najafi M, Goradel NH, Farhood B, et al. Tumor microenvironment: interactions and therapy. J Cell Physiol. 2019;234(5):5700–5721.

41. Hinshaw DC, Shevde LA. The tumor microenvironment innately modulates cancer progression. Cancer Res. 2019;79(18):4557–4566.

42. Viacava P, Bocci G, Fanelli G, et al. Microvessel density in human normal and neoplastic parathyroids. Endocr Pathol. 2006;17(2):175–181.

43. Garcia de la Torre N, Buley I, Wass JA, Jackson DG, Turner HE. Angiogenesis and lymphangiogenesis in parathyroid proliferative lesions. J Clin Endocrinol Metab. 2004;89(6):2890–2896.

44. Silva-Figueroa A, Villalobos P, Williams MD, et al. Characterizing parathyroid carcinomas and atypical neoplasms based on the expression of programmed death-ligand 1 expression and the presence of tumor-infiltrating lymphocytes and macrophages. Surgery. 2018; 164(5):960–964.

45. Hu Y, Cui M, Bi Y, et al. Immunocyte density in parathyroid carcinoma is correlated with disease relapse. J Endocrinol Invest. 2020;43(10): 1453–1461.

46. Zou X, Tang XY, Qu ZY, et al. Targeting the PDGF/PDGFR signaling pathway for cancer therapy: a review. Int J Biol Macromol. 2022; 202:539–557.

47. Arya AK, Singh P, Saikia UN, et al. Dysregulated mitogen-activated protein kinase pathway mediated cell cycle disruption in sporadic parathyroid tumors. J Endocrinol Invest. 2020;43(2):247–253.

48. Cromer MK, Starker LF, Choi M, et al. Identification of somatic mutations in parathyroid tumors using whole-exome sequencing. J Clin Endocrinol Metab. 2012;97(9):E1774–E1781.